The ground state of the Penson-Kolb-Hubbard model

1995 J. Phys.: Condens. Matter 7 5537

(http://iopscience.iop.org/0953-8984/7/28/011)

J. Phys.: Condens. Matter 7 (1995) 5537–5547. Printed in the UK

The ground state of the Penson–Kolb–Hubbard model

Bibhas Bhattacharyya and G K Roy
SSMP Division, Saha Institute of Nuclear Physics, 1/AF-Bidhannagar, Calcutta 700064, India

Received 19 December 1994, in final form 11 April 1995

Abstract. The ground state of the one-dimensional half-filled Penson–Kolb–Hubbard model (with competing single-particle and pair hoppings in the presence of on-site Coulomb repulsion) has been investigated by a real space renormalization group method. The ground state energy, energy gap, local moment and several correlation functions are studied to obtain the phase diagram. The phase diagram consists of a spin density wave (SDW) state, a superconducting (SC) phase and a quasi-metallic phase dominated by short range SC correlations for positive values of the pair hopping amplitude; when this amplitude is negative, the phase diagram contains a near-metallic commensurate charge density wave and an SC phase of pairs with centre-of-mass momentum $q = \pi$ apart from an SDW phase.

1. Introduction

The intervening years since the discovery of high-T_c cuprate superconductors [1] have brought a somewhat clearer picture of the essential characteristics of these systems. The parent (undoped) compounds are very good antiferromagnetic insulators, suggesting strong on-site Coulomb repulsion U. Neutron, muon-spin rotation and NMR experiments observe $S = \frac{1}{2}$ local moments on the Cu sites with loss of antiferromagnetic correlations as the system is doped [2]. Further increases in the hole concentration perturbs the system to favour the formation of Cooper pairs with coherence lengths of a few times the lattice spacing so that these pairs are weakly overlapping in real space; this is in marked contrast to traditional (BCS) superconductors where the number of fermions within a Cooper pair is very large. The attractive (negative-U–t, with t the nearest-neighbour single-particle hopping) Hubbard model with its zero-range instantaneous attraction has been vigorously pursued [3, 4] to describe the evolution of these systems from the Cooper pair regime to the Bose (composite boson) limit. The justification of such a model is heavily dependent on the elimination of local phonon coordinates, a situation that seems closer [5] to amorphous and highly disordered materials than high-T_c systems. The fall of T_c in this strong-coupling Bose regime ($|U|/t \gg 1$) shows an incorrect dependence [6] on U/t because a pure Hubbard-like model becomes classical in this limit; its applicability in this region thus becomes questionable. The simplest way to overcome this impasse is to use a non-local pairing interaction. The physics of these systems in the dilute 'pair' limit would then be decided primarily through the competition between single-particle hopping and localized-pair hopping (rather than pair–pair interactions), the so-called Penson–Kolb model [7]. A relatively less studied model embracing these basic features thus corresponds to the Hubbard generalization [8] of the Penson–Kolb Hamiltonian

$$H = t \sum_{\langle ij \rangle, \sigma} a_{i\sigma}^{\dagger} a_{j\sigma} + U \sum_{i} n_{i\uparrow} n_{i\downarrow} - V \sum_{\langle ij \rangle} d_i^{\dagger} d_j - \mu \sum_{i} (n_{i\uparrow} + n_{i\downarrow}) \qquad (1)$$

with the pairing V-term quadratic in on-site singlet pair creation (destruction) $d_i^\dagger = a_{i\uparrow}^\dagger a_{i\downarrow}^\dagger$ ($d_i = a_{i\downarrow}a_{i\uparrow}$) operators; $a_{i\sigma}^\dagger$ ($a_{i\sigma}$) are fermion operators, the number operator $n_{i\sigma} = a_{i\sigma}^\dagger a_{i\sigma}$ and μ is the chemical potential; $\langle ij\rangle$ represents nearest-neighbour sites on an N-site lattice. The relevant parameter space of the high-T_c systems requires $U, V > 0$. The non-local nature of V gives greater pair mobility and renders the present model essentially different from the negative-U–t Hamiltonian. As distinct from the contentious issue of the origin of the pairing mechanism, this phenomenological modelling of the pairing process has the merit of admitting different ground-state orderings in the parameter space. One can then go back to experiments for comparison and thereby identify the appropriate parameter space of these systems. A continuation of this phenomenology (postulation of unusual pairing mechanisms) is necessary before one can hope for a complete theory of high-T_c superconductivity.

It is notable that the pair-hopping term in the Hamiltonian (1), though introduced phenomenologically, is derivable from a two-body interaction term in a general tight-binding Hamiltonian [9]. The general interaction term $\langle ij|1/r|kl\rangle$ referring to the matrix element between Wannier orbitals located at sites i, j, k, l gives rise to the on-site term U for $i = j = k = l$. Similarly for $i = j$ and $k = l$ this matrix element gives the V term.

The ground state (determined by U/t, V/t) properties of the half-filled ($\mu = U/2$ by particle–hole symmetry) one-dimensional (1D) Penson–Kolb–Hubbard (PKH) model was studied by Hui and Doniach [8] (hereinafter referred to as HD) by both momentum-space renormalization-group (RG) and finite-size (exact diagonalization of finite-size cells) methods. The present work is concerned with some issues (detailed later) that remained unresolved in the HD approach. Heuristic arguments, based on exact solutions of the limiting cases (U–t and U–V models) and exact weak-coupling ($U \sim V \ll t$) results discussed in HD, indicate four types of ground state in the (U/t, V/t) phase plane: spin density wave (SDW), charge density wave (CDW), weak-coupling (BCS-type) and strong-coupling superconducting states (WSC and SSC). The phase boundaries, three of which were realized by the finite-size calculations (SDW/CDW, SDW/SSC and CDW/SSC), meet at a tricritical point $(t, U, V) \sim (1, 13.5, 10.5)$. The continuum model RG (weak-coupling expansion) of HD fails to reproduce the tricritical point and generates two additional unphysical phases: a CDW phase in the SSC region ($t \ll U < 4V/\pi$) and a phase boundary in the intermediate- and strong-coupling regimes implying a transition in the Hubbard (positive-U–t) model. Apart from these inconsistencies (noted by HD), one expects the tricritical point to be in the intermediate region ($t \sim U \sim V$) where all three (t, U, V) processes of the PKH model compete on an equal footing, but the finite-size calculations place (U, V) an order of magnitude above t. Moreover, the weak-coupling region where RG of HD can be trusted displays an SC phase not detected by the finite-size calculations. Clearly finite-size effects are very much there and if a CDW-dominated region does exist, it should be in the region $U \sim V \ll t$ rather than what HD observe. With these few observations, we proceed to explore the basic qualitative features of the PKH model for both $V > 0$ and $V < 0$ by using a simple ground-state real-space renormalization group (RSRG) method. This particular technique is known to reproduce the basic features of the ground-state properties of the 1D Hubbard model quite successfully. It can predict a metal–insulator transition at $U/t = 0$ and an antiferromagnetic SDW correlation in the insulating phase for half-filling [10, 11]. There is a sharp rise in the q transform of the SDW correlation around $q = \pi$ [10] for large values of U which bears the signature of the well known non-analytic behaviour of the correlation function near $q = 2k_F$ (where the Fermi momentum $k_F = \pi/2$ for half-filling). It is, therefore, of interest to know the extent to which this approach (within a first-order theory) is able to capture the essential aspects of the ground state of the PKH model without bringing in the unphysical phases referred to above.

2. RSRG equations

The present Hamiltonian has several symmetries apart from the particle–hole symmetry (for half-filling) mentioned earlier. The total spin S, the z-component S_z of the total spin and the total number of particles ν are conserved quantities. The model also possesses a spin-reversal symmetry in the absence of a polarizing field. We shall be using these symmetries in constructing the RG formalism.

In the present RG scheme [10, 11] the lattice is partitioned into three-site blocks. The block Hamiltonian is then diagonalized exactly. Only four low-lying states in the subspaces $\{S = S_z = 0, \nu = 2\}$, $\{S = S_z = \frac{1}{2}, \nu = 3\}$, $\{S = -S_z = \frac{1}{2}, \nu = 3\}$ and $\{S = S_z = 0, \nu = 4\}$ are retained. These are identified with the renormalized $|0\rangle$, $|\uparrow\rangle$, $|\downarrow\rangle$ and $|\uparrow\downarrow\rangle$ states respectively. Of these the first and fourth are connected by particle–hole symmetry while the second and third are connected by spin-reversal symmetry. The inter-block part of the Hamiltonian is then renormalized within this truncated basis to yield the following first-order RG equations:

$$U' = U + 2(E_2 - E_3) \qquad V' = \left(\tfrac{1}{2}a_2^2 + \sqrt{2}a_3a_4\right)^2 V$$

$$t' = \left[\frac{1}{2\sqrt{2}}(a_2b_1 + a_1b_2) + \frac{3}{2\sqrt{6}}a_2b_3 + \frac{1}{2\sqrt{2}}a_3b_2 + \tfrac{1}{2}a_4b_2\right]^2 t \tag{2}$$

$$\mu' = E_2 - E_3 + \mu = U'/2$$

where E_2 and E_3 are the lowest eigenvalues, and (a_1, a_2, a_3, a_4) and (b_1, b_2, b_3) are the corresponding eigenvectors of the matrices

$$M_2 = \begin{pmatrix} 0 & \sqrt{2}t & 0 & 0 \\ \sqrt{2}t & 0 & \sqrt{2}t & 2t \\ 0 & \sqrt{2}t & U & -\sqrt{2}V \\ 0 & 2t & -\sqrt{2}V & U \end{pmatrix} \qquad M_3 = \begin{pmatrix} U & \sqrt{2}t & 0 \\ \sqrt{2}t & U - V & \sqrt{6}t \\ 0 & \sqrt{6}t & 0 \end{pmatrix}$$

respectively. M_2 and M_3 are the irreducible parts of the block Hamiltonian containing the lowest eigenvalues in the subspaces $\nu = 2$ and $\nu = 3$ respectively. These recursion relations relate the renormalized parameters (U', V', t') at the nth stage with the previously obtained iterated values.

We have computed the ground-state energy per site E from the relation [10]

$$E = \sum_{n=1}^{\infty}(E_2^{(n)} - 2\mu^{(n)})/3^n + U/2.$$

The local moment L, defined by $L = \langle S_i^2 \rangle$, can also be computed recursively from

$$L = \tfrac{3}{4}a_2^2 + (b_1^2 + b_3^2 - a_2^2)L'.$$

We also compute the q-transform of the spin–spin, density–density and pair–pair correlation functions to study SDW, CDW and SC orderings. Such correlation functions are defined as

$$C(q) = N^{-1}\sum_{ij}\langle A_i^{\dagger}A_j\rangle \exp[\mathrm{i}q(R_i - R_j)]$$

where $A_i = (n_{i\uparrow} - n_{i\downarrow})$, $(1 - n_{i\uparrow} - n_{i\downarrow})$ or d_i for SDW, CDW and SC correlations respectively; R_i refers to the position of the ith site. Recursion of such correlation functions is fairly straightforward [10]. The recursion relations are of the general form

$$C(q) = \alpha(q) + \beta(q)L' + \gamma(q)C'(3q) \tag{3}$$

where $\alpha(q)$, $\beta(q)$ and $\gamma(q)$ are quantities depending on q, U/t and V/t. The explicit forms of these quantities in terms of a_i and b_i are given in the appendix.

3. Phase diagram

The phase diagram in the $(U/t,\ V/t)$ plane of figure 1 is constructed from the trajectories of the running coupling parameters $(U'/t',\ V'/t')$ appearing in the recursion relations of (2). The nature of ordering in a particular phase is obtained by studying appropriate correlation functions, energy, energy gap and local moment. For $V > 0$ the phase diagram consists of an antiferromagnetic SDW phase, a superconducting (SC) phase and a nearly metallic phase with short-range superconducting (SRS) correlations. In the case $V < 0$, there appear a quasi-metallic commensurate CDW phase and an η-paired (pairs with centre-of-mass momentum π) SC phase (η-SC) apart from an SDW one.

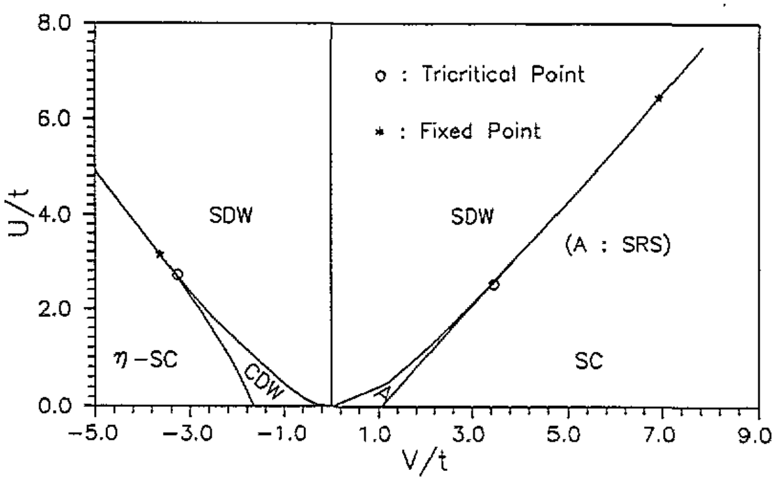

Figure 1. Phase diagram of the 1D PKH model for half-filling. The enclosed region marked 'A' shows the SRS phase. SDW: spin density wave; CDW: charge density wave; SRS: quasi-metallic phase with short-range pairing correlation; SC: superconducting phase; η-SC: η-paired SC phase with pairs of centre-of-mass momentum π.

Any point in the SDW region flows into the stable fixed point $(\infty, 0)$ under RG iterations. Points in both the SRS region and the CDW region go to the stable fixed point $(-\infty, 0)$ under RG flow. On the other hand, the points in the SC regions flow to $(-\infty, \infty)$ or $(-\infty, -\infty)$ for $V > 0$ or $V < 0$ respectively (figure 2).

The SDW boundary is the line of zeros of the energy gap U_∞ (the limiting value U' reaches after infinite iterations while t' and V' separately go to zero). The SDW region $(U_\infty > 0)$ is characterized by the opening of a single-particle excitation gap in the charge

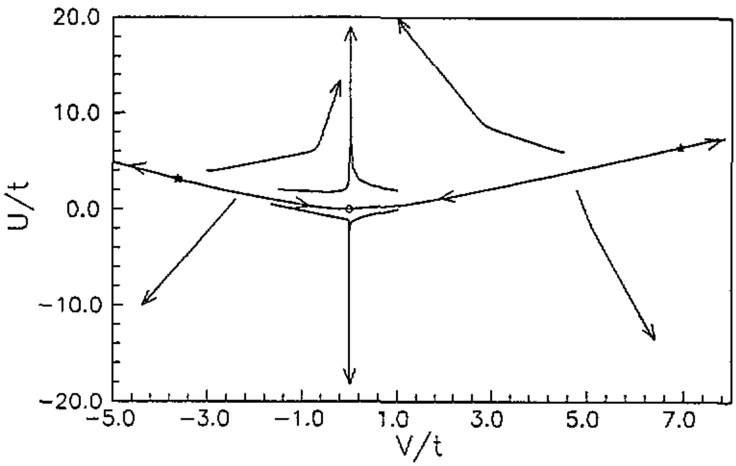

Figure 2. RG flow diagram of the 1D PKH model for half-filling. $*$: the unstable FP (fixed point) on the SDW boundaries. o: stable free-fermion FP at (0, 0).

sector, while below this boundary a gap in the spin sector ($U_\infty < 0$) emerges. That the region where $U_\infty > 0$ corresponds to an SDW phase is evident from the plot of the SDW correlation $C_{SDW}(q)$ against U/t (figure 3). $C_{SDW}(q)$ increases to large values for $q = \pi$ in this region (for both $V > 0$ and $V < 0$) implying an antiferromagnetic order. An unstable fixed point (marked $*$) appears at $\simeq$ (6.448, 6.930) on this boundary for $V > 0$, the linearized RG matrix having eigenvalues (1.524, 4.586) with eigenvectors (0.825, 0.645) and (0.822, −0.570) respectively, the latter defining two critical surfaces near this point on the SDW line. For $V < 0$, a similar unstable fixed point (FP) appears on the SDW boundary at $\simeq$ (3.145, −3.617) which also separates two critical lines on this SDW boundary (figure 1). The metallic critical lines extend from the unstable FPs to the free-fermionic stable FP (0, 0); all points on the two metallic critical lines flow to (0, 0) under RG iterations. The other part of the SDW line, beyond the unstable FP, flows to the stable FP (∞, ∞) or (∞, $-\infty$) for $V > 0$ or $V < 0$ respectively with $U/|V| \to 4\sqrt{2}/5$ ($<4\ \pi$, the exact value). This follows from (2) by setting $U > |V|$ and letting $t \to 0$.

In the enclosed regions below the SDW boundary, namely the SRS and the CDW phases, the gap $|U_\infty| \gtrsim 0$ (figure 4). This shows the nearly metallic nature of these phases in which single-particle hopping dominates over pair hopping with V/t scaling to zero. Comparing the SC and the CDW correlations, $C_{SC}(q)$ and $C_{CDW}(q)$, we find that the difference

$$D(U/t, V/t) = 2C_{SC}(q = 0) - C_{CDW}(q = \pi) \geqslant 0$$

throughout the SRS region (the factor 2 before C_{SC} arises because $d_i^\dagger$, d_i and $(n_{i\uparrow}+n_{i\downarrow}-1)/2$ form a spin algebra); the equality holds only at (0, 0). Figure 5 illustrates this comparison for $U = 0$; identical remarks apply in this region for other U values. There is no SC ordering in the SRS zone as it is a single-particle-hopping-dominated region. Such a quasi-metallic phase with short-range pairing correlations also shows up in a Gutzwiller variational approach [12], but it does not come out of the finite-size calculations of HD. On the other hand, there is CDW ordering in the negative-V sector; $C_{CDW}(q = \pi)$ dominates over other correlations, rapidly increases as the CDW/η-SC boundary (on which it peaks) is approached and then decays quickly in the η-SC zone (in contrast to its behaviour in the SC region where it never acquires appreciable values compared to the free-fermion value).

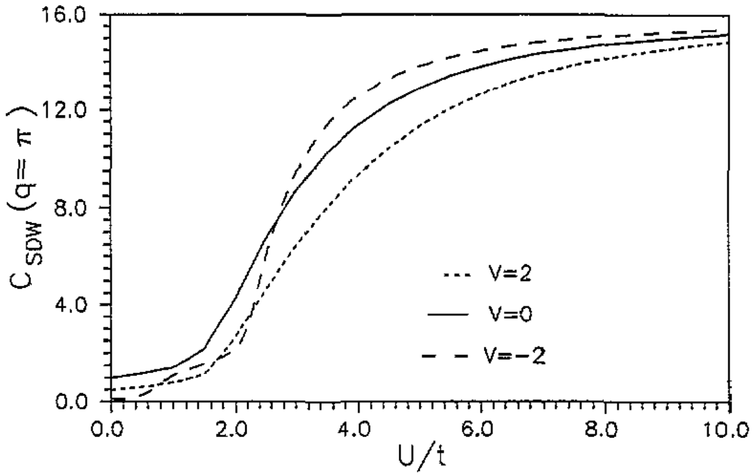

Figure 3. Plots of the SDW correlation functions $C_{SDW}(q = \pi)$ against U/t for different V/t $(t = 1.0)$.

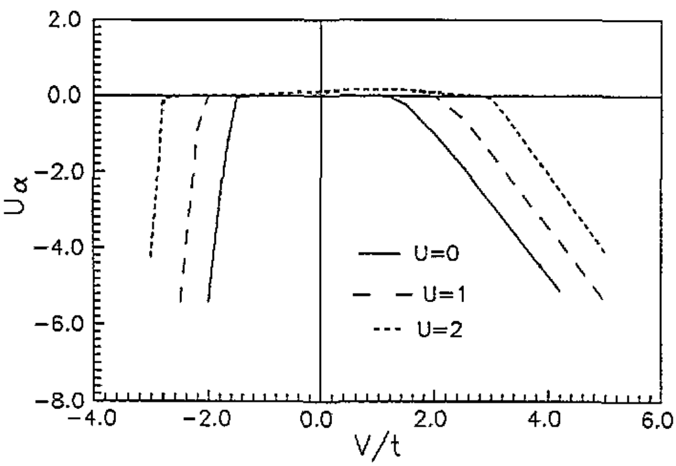

Figure 4. U_∞ against V/t parametrized by U/t $(t = 1.0)$. The fall of U_∞ is much sharper in the $V < 0$ sector compared to that in the $V > 0$ region.

It may, however, be noted that since the CDW region is bounded, the ordering in it is never complete as distinct from the SDW and SC phases in the large U/t and $|V|/t$ limits respectively.

It is very striking that for both the CDW and SRS phases the RG flow goes to the negative-U Hubbard FP $(-\infty, 0)$. The negative-U Hubbard model possesses degenerate CDW $(q = \pi)$ and SC $(q = 0)$ channels for half-filling [4]. But in these two regions of the PKH model (which flow to the same FP under RG) this degeneracy is removed and in ways opposing each other. The reason behind this is the short-range pairing fluctuation competing with the single-particle hopping t. This effect enters the RG calculations through the first few iterations necessary to get rid of the pair hopping amplitude V to reach the FP $(-\infty, 0)$. It is also very interesting to observe the sharp difference in the effect of V in the two regimes $V > 0$ and $V < 0$. This indicates that the nature of the competition between

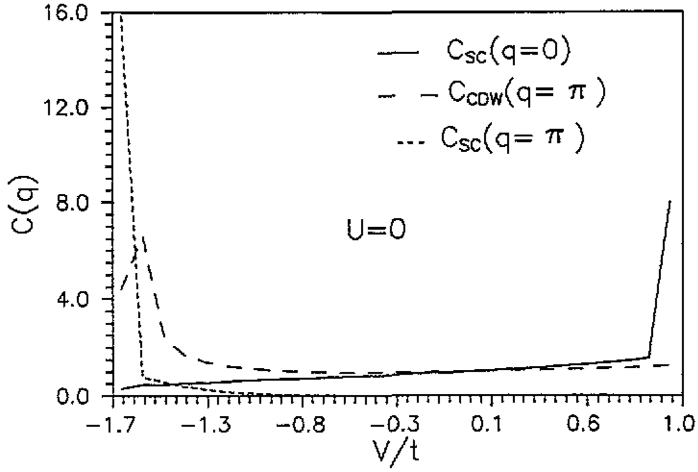

Figure 5. Comparative plots of CDW and SC correlation functions: $C_{CDW}(q = \pi)$, $2C_{SC}(q = 0)$ and $2C_{SC}(q = \pi)$ against V/t for $U/t = 0$.

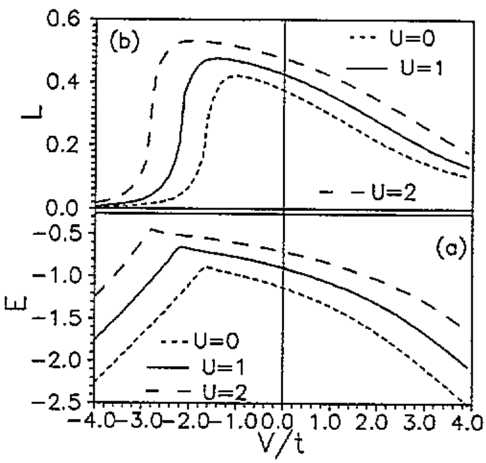

Figure 6. Plots of (*a*) the ground-state energy/site E and (*b*) the local moment L against V/t for different U/t ($t = 1.0$). The peak in the energy corresponds to a sharp fall in the local moment, signalling the onset of the composite boson phase.

V and t in the SRS phase is different from that in the CDW phase. In fact, this becomes evident from the plot of the ground-state energy (per site) E against V/t (figure 6). The energy curve is asymmetric around $V = 0$. It is noticeable that the V term favours the band effect to lower the energy in the $V > 0$ sector, i.e. in the SRS phase. On the other hand, for $V < 0$, the pairing term increases the energy (compared to that for $V = 0$) by opposing the single-particle hopping. This gives rise to the fact that U/t scales to infinity much faster in the SDW phase of $V < 0$ sector compared to that for $V = 0$ case; however, this rate is slower for the $V > 0$ SDW region. This is why, in the SDW ordered phase, we find that $C_{SDW}(q = \pi)$ for $V < 0$ takes larger values than that for $V = 0$ while the $V > 0$ curve lies below it (figure 3).

As the SC region ($V > 0$) is approached across the SRS/SC boundary, the pair hopping mechanism begins to dominate over the single-particle hopping since $V/t \to \infty$ under RG iterations (figure 2). U_∞ suddenly takes on large negative values (whose magnitude gives the gap in the spin sector; figure 4) indicating the formation of tightly bound pairs. It is found that the pairing correlation $C_{SC}(q)$ blows up in this phase for $q = 0$ (figure 7) as $V/t \to \infty$; other q values give vanishingly small contribution. This indicates an SC pairing out of pairs with centre of mass at rest.

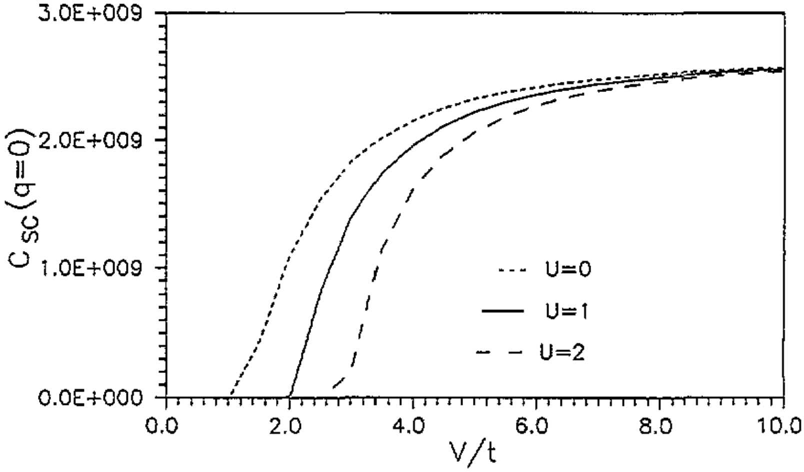

Figure 7. SC correlation functions $C_{SC}(q = 0)$ against V/t for different U/t $(t = 1.0)$.

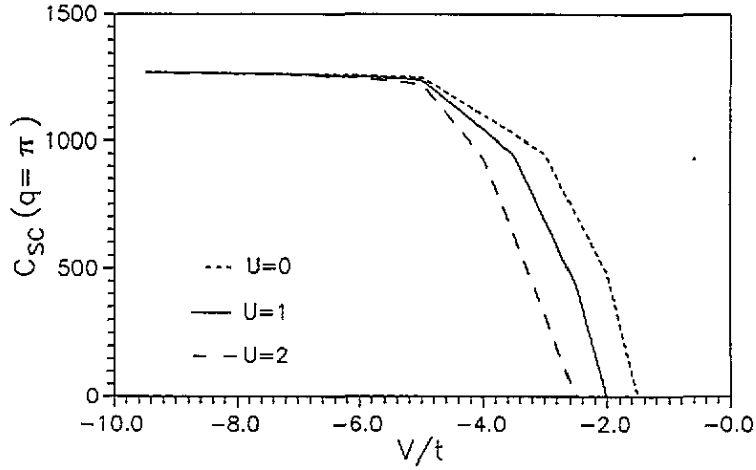

Figure 8. SC correlation functions $C_{SC}(q = \pi)$ against V/t for different U/t $(t = 1.0)$.

A similar situation occurs as we move inside the η-SC region across the CDW/η-SC boundary: $V/t \to -\infty$. Consequently the pairing correlation $C_{SC}(q)$ starts dominating over the CDW correlation. But the role of the pairing interaction is distinctly different from that in the $V > 0$ case, as noted earlier. $C_{SC}(q)$ takes on large values (figure 8) for $q = \pi$ (instead of $q = 0$ for $V > 0$). This kind of pairing with centre-of-mass momentum $q = \pi$ is often referred to as η-pairing [13]. In the present context, it is not a surprising result.

The q-transform of the pairing term, $-2V\cos(q_1+q_2)$ where q_1 and q_2 are the momenta of the interacting electrons, has a maximum negative value when $q_1+q_2=\pi$ for $V<0$.

The three phase boundaries meet at a tricritical point for both $V>0$ and $V<0$; for $V>0$ this tricritical point is at $\simeq (t:1.0, U:3.0, V:3.85)$ while for $V<0$ it is at $\simeq (t:1.0, U:3.0, V:-3.51)$. It is notable that t, U and V are of the same order of magnitude at the tricritical point as expected (this was not so in the results of HD). Moreover, the absolute values of t, U and V are nearly same for both $V>0$ and $V<0$.

The phase transitions from a near-metallic state to an SC phase are different in nature for positive V and negative V. For $V>0$, we find that this transition corresponds to the development of long-range order in some particular correlation (e.g. the $q=0$ SC correlation jumps across the SRS/SC boundary). The variation of the local moment across this transition (at $V/t\simeq 1.04$ for $U=0$, the so-called Penson–Kolb point) is also quite smooth (figure 6). In fact it is hard to detect this transition without referring to the RG flow. But the transition in the negative-V sector is clearly accompanied by a change in the nature of ordering (e.g. from CDW to an η-paired SC). The local moment also shows a sharp fall at this transition (figure 6) which, for $U=0$, takes place at $V/t\simeq -1.65$ (note that the energy curve peaks exactly at this point). This particular behaviour in the local moment plot shows that the evolution of the SC phase towards a hard-core boson phase (of tightly bound pairs) is gradual for $V>0$; within the SC phase the weights of the configurations containing single occupancies in the wavefunction decrease asymptotically with increasing V/t. In contrast, one reaches the hard-core boson regime immediately after crossing the CDW/η-SC boundary for $V<0$. This feature was present in the field theoretic analysis of Affleck and Marston [14] who concluded that a true pairing transition occurs only in the negative-V sector of the Penson–Kolb model (the PKH model without the U term).

4. Conclusion

In conclusion, we have studied the 1D PKH model for half-filling using a real-space RG technique for both $V>0$ and $V<0$. This technique uses a repeated renormalization of a product wavefunction incorporating exact solutions of the model in a three-site cell. Therefore, in contrast to the weak- and strong-coupling expansions, the method is expected to work reasonably well over the entire regime of the parameter space. Moreover, this approach incorporates fluctuations beyond the mean-field analysis which is essential for the study of low-dimensional systems. It is well known that this method suffers from the fact that the renormalization of the off-diagonal quantities (e.g. t or V) are not very accurate (within the framework of first-order RG [11]) and the reason behind this has recently been addressed [15]. But apart from its quantitative precision, this technique succeeded in bringing out the essential qualitative features of interacting fermion models [10, 11, 16].

We find that the phase diagram for the PKH model consists of an SDW phase, an SC region and a quasi-metallic phase with short-range SC correlations for $V>0$ while for $V<0$ it contains an η-paired SC and a near-metallic CDW phases besides an SDW phase. Also the local moment and the ground-state energy computed from the RSRG provide some interesting information about the competition between the two distinct hopping processes. It is worth noting here again that the unphysical phases (referred to in section 1) generated by the momentum space RG in the intermediate- to strong-coupling regime are absent in the present approach. It is thus expected to work better in this regime where the high-T_c superconductors are likely to reside [3].

We believe it would be worthwhile to study the convergence property of the present approach as a function of block size; this should be faster than finite-size calculations for the simplest one (three-site cell) has revealed the essential properties of the PKH model. Identification of the appropriate order parameter for the SRS phase would constitute definite progress; if such an order parameter does exist, its corresponding correlation function should dominate in the SRS phase and then decay on entering the SC region. The nature of elementary excitations in the different phases may help in this matter. Finally, this study needs to be extended to higher dimensions for comparison with experiment.

Appendix

The quantities $\alpha(q)$, $\beta(q)$ and $\gamma(q)$ in (3) are given as follows.

For SDW correlation:

$$\alpha(q) = e_7 + \tfrac{4}{3}e_3\cos(q) + \tfrac{2}{3}\cos(2q)$$
$$\beta(q) = \tfrac{4}{9}[e_8 - e_1^2 - 2e_2^2 + 4(e_4 - e_1e_2)\cos(q) + 2(e_6 - e_2^2)\cos(2q)]$$
$$\gamma(q) = \tfrac{1}{3}[e_1^2 + 2e_2^2 + 4e_1e_2\cos(q) + 2e_2^2\cos(2q)]$$

where

$$e_1 = b_1^2 - b_3^2/3 \qquad e_2 = b_2^2/2 + 2b_3^2/3 \qquad e_3 = -a_2^2/2$$
$$e_4 = -2b_3^2/3 + a_2^2/2 \qquad e_5 = -a_1^2 \qquad e_6 = b_3^2/3 + a_1^2$$
$$e_7 = 2(a_1^2 + a_2^2)/3 \qquad e_8 = 1 + 2(b_3^2 - a_1^2 - a_2^2).$$

For CDW correlation:

$$\alpha(q) = \tfrac{1}{3}[d_7 - d_1^2 - 2d_2^2 + 4(d_3 - d_1d_2)\cos(q) + 2(d_5 - d_2^2)\cos(2q)]$$
$$\beta(q) = \tfrac{4}{9}[d_8 + d_1^2 + 2d_2^2 + 4(d_4 + d_1d_2)\cos(q) + 2(d_6 + d_2^2)\cos(2q)]$$
$$\gamma(q) = \tfrac{1}{3}[d_1^2 + d_2^2 + 4d_1d_2\cos(q) + 2d_2^2\cos(2q)]$$

where

$$d_1 = a_1^2 + a_3^2 - a_4^2 \qquad d_2 = a_2^2/2 + a_4^2 \qquad d_3 = -a_4^2$$
$$d_4 = -b_2^2/2 + a_4^2 \qquad d_5 = -a_3^2 + a_4^2 \qquad d_6 = -b_1^2 + a_3^2 - a_4^2$$
$$d_7 = 1 + 2(a_3^2 + a_4^2) \qquad d_8 = 1 - 2(b_3^2 + a_3^2 + a_4^2).$$

For SC correlation:

$$\alpha(q) = \tfrac{1}{3}[2f_3 + f_6 + f_1^2 + f_2^2/2 - \tfrac{1}{2} + 2(f_1 + f_6 - f_4 + f_1f_2)\cos(q) + (2f_3 + f_1^2)\cos(2q)]$$
$$\beta(q) = \tfrac{4}{9}[2f_5 + f_7 - 2f_3 - f_6 - f_1^2 - f_2^2/2 + \tfrac{1}{2} + 2(f_4 + f_7 - f_1 - f_6 - f_1f_2)\cos(q)$$
$$- (2f_3 + 2f_5 - f_7 + f_1^2)\cos(2q)]$$
$$\gamma(q) = \tfrac{1}{3}[2f_1^2 + f_2^2 + 4f_1f_2\cos(q) + 2f_1^2\cos(2q)]$$

where

$$f_1 = a_2^2/2 + \sqrt{2}a_3a_4 \qquad f_2 = -a_1^2 + a_3^2 \qquad f_3 = a_3^2/2$$
$$f_4 = a_2^2/2 + a_4^2 \qquad f_5 = b_1^2/2 + b_2^2/4 \qquad f_6 = a_4^2 \qquad f_7 = b_2^2/2.$$

References

[1] Bednorz J G and Müller K A 1986 *Z. Phys.* B **64** 88
[2] Fukuyama H, Maekawa S and Malozemoff A (ed) 1989 *Strong Correlation and Superconductivity* (Berlin: Springer)
[3] Randeria M *et al* 1992 *Phys. Rev. Lett.* **69** 2001
Scalettar R T *et al* 1989 *Phys. Rev. Lett.* **62** 1407
Belkhir L and Randeria M 1992 *Phys. Rev.* B **45** 5087
[4] Luo J and Bickers N E 1993 *Phys. Rev.* B **48** 15 983
[5] Anderson P W 1975 *Phys. Rev. Lett.* **34** 953
[6] Nozières P and Schmitt-Rink S 1985 *J. Low. Temp. Phys.* **59** 195
[7] Penson K A and Kolb M 1986 *Phys. Rev.* B **33** 1663; 1986 *J. Stat. Phys.* **44** 129
[8] Achille H and Doniach S 1993 *Phys. Rev.* B **48** 2063
[9] Hubbard J 1963 *Proc. R. Soc.* A **276** 238
[10] Hirsch J E 1980 *Phys. Rev.* B **22** 5259
[11] Dasgupta C and Pfeuty P 1981 *J. Phys. C: Solid State Phys.* **14** 717
[12] Fazekas P *Preprint*
[13] Yang C N 1989 *Phys. Rev. Lett.* **63** 2144
[14] Affleck I and Marston J B 1988 *J. Phys. C: Solid State Phys.* **21** 2511
[15] White S R and Noack R M 1992 *Phys. Rev. Lett.* **68** 3487
[16] Perez-Conde J and Pfeuty P 1993 *Phys. Rev.* B **47** 856
Yi J, Zhang L and Canright G S 1994 *Phys. Rev.* B **49** 15 920